Supporting information for

Thermoreversible magnetic nanochains

Jiří Mikšátko, David Aurélio, Petr Kovaříček, Magdalena Michlová, Miroslav Veverka, Michaela Fridrichová, Irena Matulková, Martin Žáček, Martin Kalbáč, Jana Vejpravová**

* E-mail: martin.kalbac@jh-inst.cas.cz, jana@mag.mff.cuni.cz

Contents

Characterization methods 2

Hydrothermal synthesis and characterization of $CoFe_2O_4$ NPs 2

Ligand synthesis and characterization 4

Ligand exchange protocol and characterization of functionalized NPs 7

NPs functionalized with 11-maleimidoundecanoic acid (Particles A) 7

NPs functionalized with 11-(furfurylureido)undecanoic acid (Particles B) 8

Model Diels-Alder reaction 10

Diels-Alder reaction between the functionalized cobalt ferrites 12

DRIFTS spectra after magnetic-field-unassisted reaction 12

Diels-Alder reaction in the MF 12

DRIFTS spectra after magnetic-field-assisted reaction 13

Retro-Diels-Alder 13

HRTEM images after magnetic-field-(un)assisted Diels-Alder and *retro*-Diels-Alder reaction 14

Magnetic measurements and properties 16

Powder X-ray diffraction 20

References 20

Characterization methods

^{1}H, ^{13}C and 2D NMR spectra were recorded on Varian Mercury 300 Plus 300 MHz NMR with 2-channel broadband Mercury Plus console, Varian 300 H/F/X PFG tunable probe and VNMRJ workstation. Chemical shifts are reported in ppm and referenced to the solvent residual signal. Mass spectra were recorded on Advion expression^{L} (CMS-L model) with an atmospheric pressure interface and ESI or APCI ionization sources, hexapole ion transfer region, single-quadrupole mass analyzer (range *m*/*z* 10 – 2000) and electron multiplier detector with a high energy dynode and switchable voltage of +/-10 kV. The infrared spectra were recorded using DRIFTS technique (dispersion of the powderized sample in KBr) on a Nicolet 6700 FTIR spectrometer with 2 cm^{-1} resolution and Happ-Genzel apodization in the 400 – 4000 cm^{-1} region. The resulting NPs were characterized using TGA-MS Netzsch STA449 F1 Jupiter equipped with Netzsch QMS 403 C Aelos mass detector (oxygen atmosphere) and DLS Zetasizer Nano Malvern. The HRTEM images were acquired on a JEOL JEM-2100Plus microscope with acceleration voltage 200 kV. The droplets of samples (7 µL) were deposited on carbon coated copper grids (300 mesh, SPI supplies #03D00931) and left to dry spontaneously in air. The picture analysis of the images was carried out using ImageJ 1.52a. The magnetic properties were measured by using a Physical Property Measurement System (Quantum Design, Inc.; 6000 model series) with the Vibrating Sample Magnetometer (VSM, Quantum Design, Inc.; P525 model) option, or a Magnetic Property Measurement System, Superconducting Quantum Interference Device (SQUID, MPMS7XL, Quantum Design, Inc.). In both systems, the temperature range used was from 2 K up to 350 K for the magnetic susceptibility measurements, and a field sweep from -7.0 T to 7.0 T for the magnetic isotherm assessment.

Hydrothermal synthesis and characterization of $CoFe_2O_4$ NPs

Iron(III) nitrate nonahydrate (≥96 %, Sigma-Aldrich), cobalt(II) nitrate hexahydrate (≥96 %, Sigma-Aldrich), oleic acid (≥99 %, Sigma-Aldrich), sodium hydroxide (pure, Merck). All chemicals were used without any further purification. NPs were synthesized in Berghof DAB-2 autoclave with 40 mL teflon liner.

$CoFe_2O_4$ NPs were prepared *via* hydrothermal synthesis.[2] A transparent solution of sodium oleate was prepared by dissolving of NaOH (10 mmol, 0.400 g) in 2 mL of distilled water and

addition of ethanol (10 mL) and oleic acid (0.708 mmol, 2 g) with vigorous stirring. Iron(III) nitrate nonahydrate (2 mmol, 0.808 g) and cobalt(II) nitrate hexahydrate (1 mmol, 0.291 g) were dissolved in 20 mL of distilled water and added to the intensely stirred oleate. The dark brown mixture was immediately transferred to an autoclave with a teflon tube and placed into a preheated oven (200 °C, 11 hours). Afterwards, the reactor was allowed to cool down to room temperature. The clear aqueous phase was removed from the reaction mixture and the dark colored oleic phase containing NPs was subjected to 4 cycles of cleaning procedure (dispersion in 10 mL of *n*-hexane, 30s of sonication, precipitation by 15 mL of ethanol, centrifugation at 4500 rpm for 5 minutes, removal of the liquids and re-dispersion of NPs in *n*-hexane). In order to remove larger aggregates of the NPs, the final dispersion was centrifuged at 4500 rpm for 5 minutes and the sediment was separated. **DLS**: 10.99 ± 0.13 nm. **TGA**: 21.6 wt % of oleic acid.

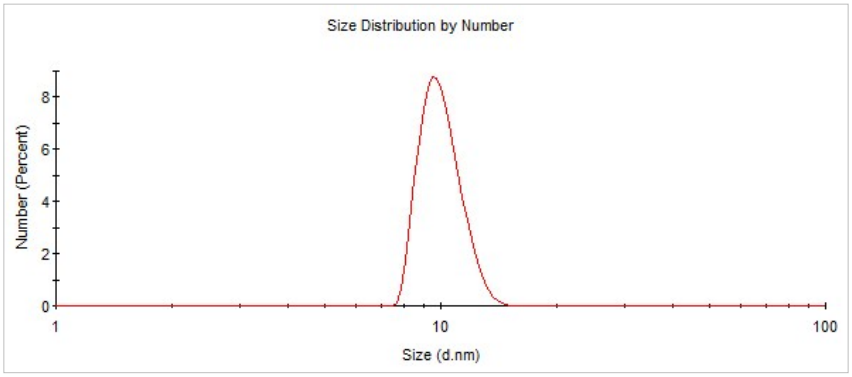

Figure S1. DLS spectrum of CoFe2O4 NPs (*n*-hexane, 298 K).

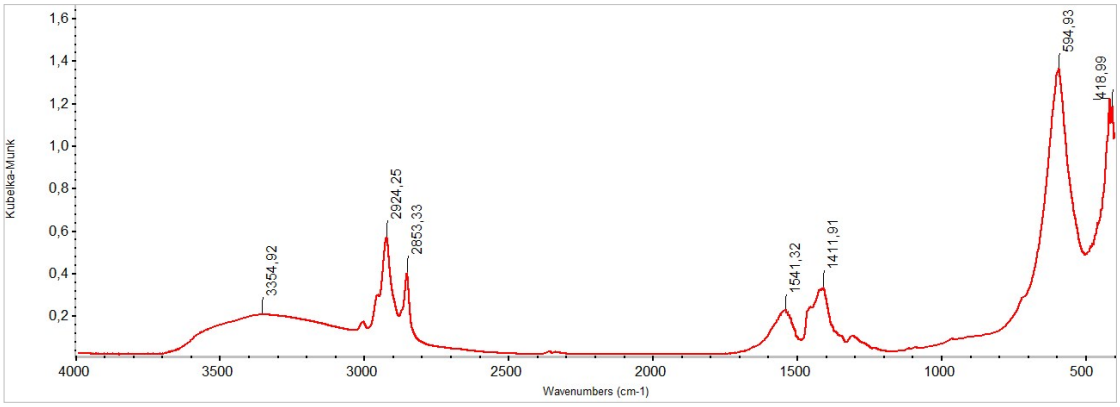

Figure S2. DRIFTS spectrum of cobalt ferrites coated with oleic acid (KBr, 298 K, cm^{-1}).

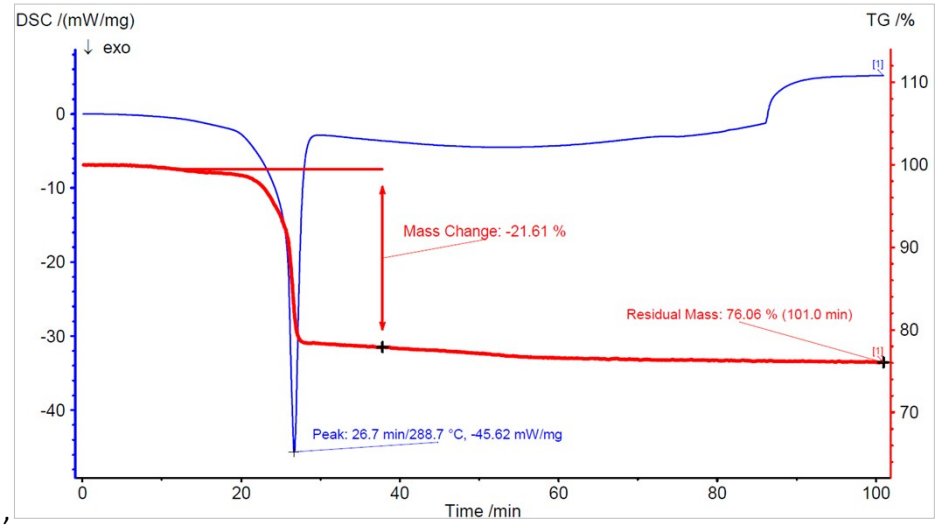

Figure S3. TGA curve of CoFe2O4 NPs (oxygen atmosphere).

Ligand synthesis and characterization

11-Maleimidoundecanoic acid (95 %), 11-aminoundecanoic acid (97 %) and furfuryl isocyanate (97 %) were purchased from Sigma-Aldrich and used as received.

11-(Furfurylureido)undecanoic acid. 11-Aminoundecanoic acid (12.2 mmol, 2.45 g) and furfuryl isocyanate (12.2 mmol, 1.50 g) were mixed in an acetonitrile (10 mL) and methanol (20 mL) mixture. Upon heating at reflux, the poorly soluble acid starts to dissolve. When cooled down to room temperature, the first precipitate is the unreacted 11-aminoundecanoic acid which was removed by filtration. The filtrate was then precipitated with ethanol and the pure product was collected by filtration (1.16 g, 29 %). **^{1}H-NMR** (300 MHz, *d*6-DMSO): δ(ppm) = 11.96 (br s, 1H, COO-*H*), 7.52 (dd, 1H, *J* = 1.8, 0.9 Hz, Fur-*H*), 6.35 (dd, 1H, *J* = 3.2, 1.8 Hz, Fur-*H*), 6.15 (dd, 1H, *J* = 3.2, 0.9 Hz, Fur-*H*), 6.14 (overlaped, 1H, Fur-CH_2-N-*H*), 5.85 (t, 1H, *J* = 5.6 Hz, –CH_2-N-*H*), 4.15 (d, 2H, *J* = 5.9 Hz, Fur-CH_2-NH), 2.95 (q, 2H, *J* = 6.5 Hz, –CH_2-NH), 2.16 (t, 2H, *J* = 7.4 Hz, –CH_2-COOH), 1.53-1.39 (m, 2H, –CH_2–), 1.38-1.26 (m, 2H, –CH_2–), 1.26-1.18 (m, 12H, –CH_2–). **^{13}C-NMR** (75 MHz, *d*6-DMSO): δ(ppm) = 175.0, 158.1, 154.2, 142.2, 110.8, 106.5, 39.9 (overlaped with the signal of solvent), 36.8, 34.1, 30.4, 29.4, 29.3, 29.2, 29.1, 29.0, 26.8, 24.9. **IR** (KBr) ν(cm^{-1}) = 3325 (m, NH), 3116 (w, CH), 2912 (m, CH_2), 2845 (m, CH_2), 1709 (m, ureido C=O), 1610 (s, carboxyl C=O), 1581 (s, C=C), 900 (m, CH), 808 (s, CH). **MS** (APCI$^-$) ($C_{17}H_{28}N_2O_4$) m/z calcd. 323.2 [M-H]$^-$, found m/z 322.8 [M-H]$^-$.

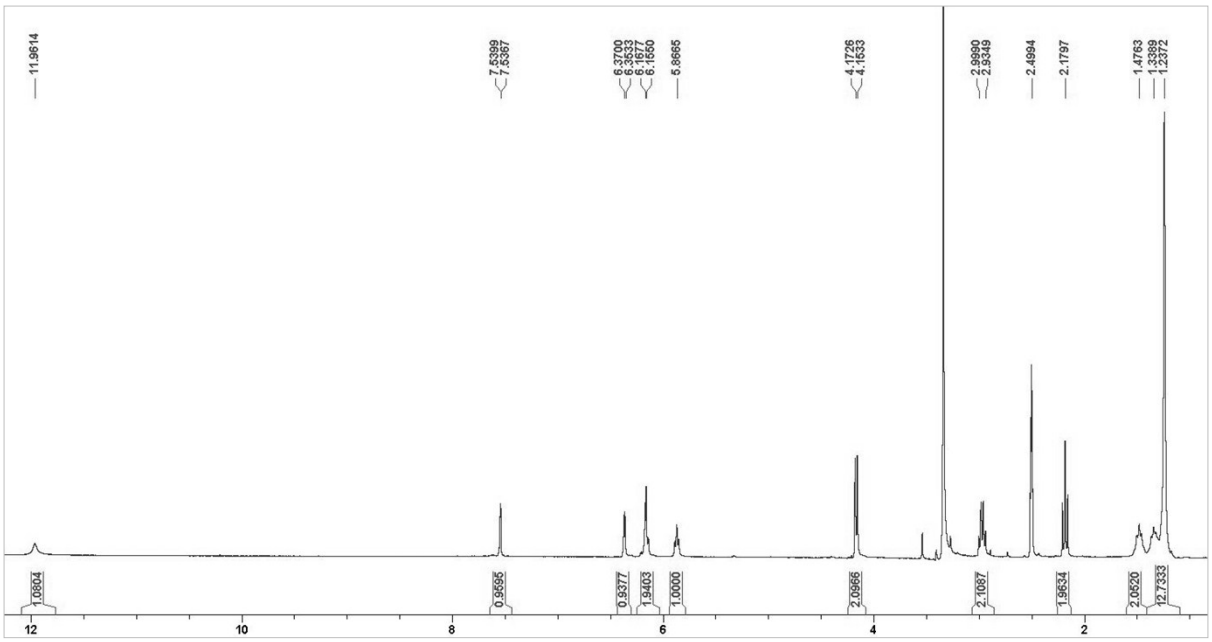

Figure S4. ^{1}H NMR of 11-(furfurylureido)undecanoic acid with a doublet at 4.15 ppm (*J*=5.9 Hz) corresponding to the methylene group between the furan ring and NH group of the formed ureido function, and quartet at 2.95 ppm of –CH_2– adjacent to the second NH group (300 MHz, *d*6-DMSO, 298 K, ppm).

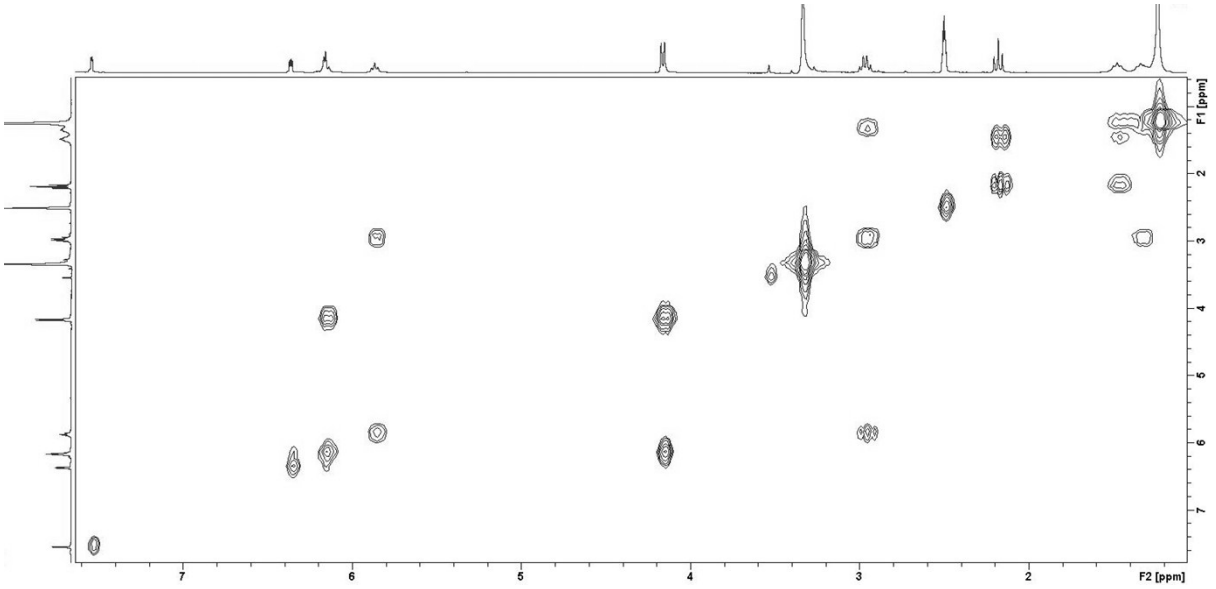

Figure S5. 2D COSY of 11-(furfurylureido)undecanoic acid revealing the contacts of the doublet (4.15 ppm) and quartet (2.95 ppm) with the corresponding NH groups (300 MHz, *d*6-DMSO, 298 K, ppm).

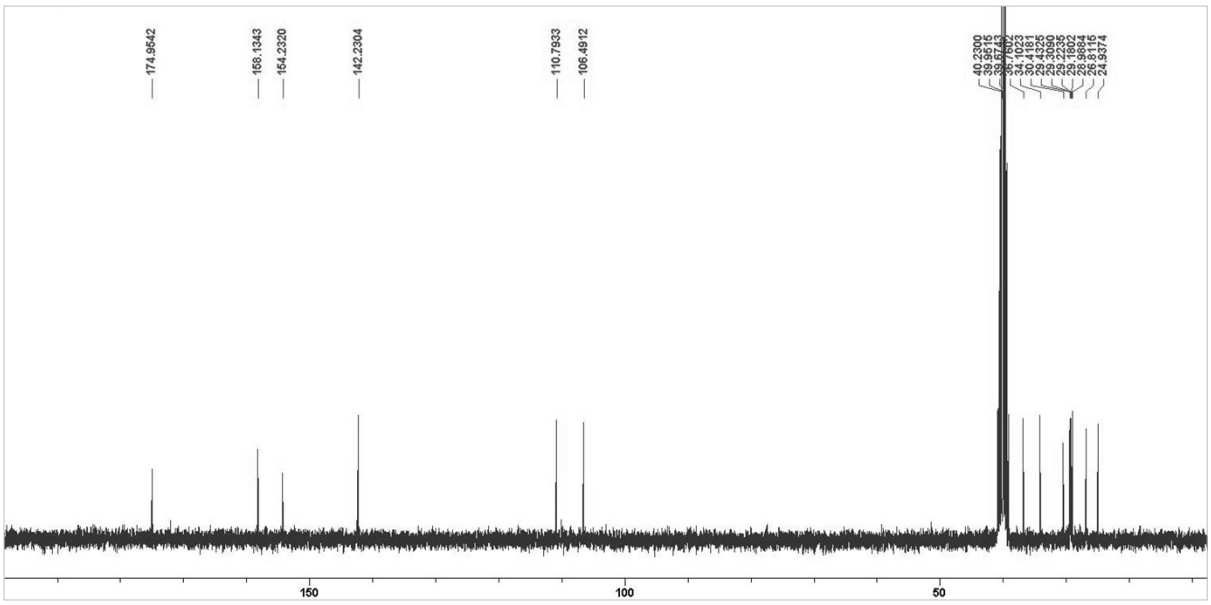

Figure S6. ^{13}C NMR of 11-(furfurylureido)undecanoic acid (75 MHz, *d*6-DMSO, 298 K, ppm).

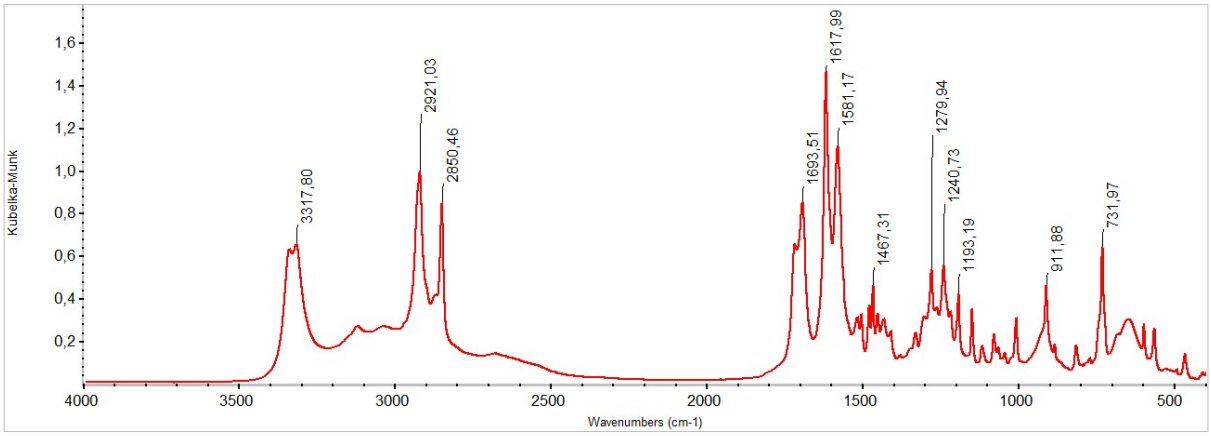

Figure S7. DRIFTS spectrum of 11-(furfurylureido)undecanoic acid showing characteristic NH stretching bands around 3320 cm^{-1} together with C=O ureido stretching bands at around 1700 cm^{-1}. In addition, besides the clear presence of –CH2– stretching, the 2-substituted furan ring is confirmed by three bands at around 915-800 cm^{-1} originated from a C-H out-of-plane deformation (KBr, 298 K, cm^{-1}).

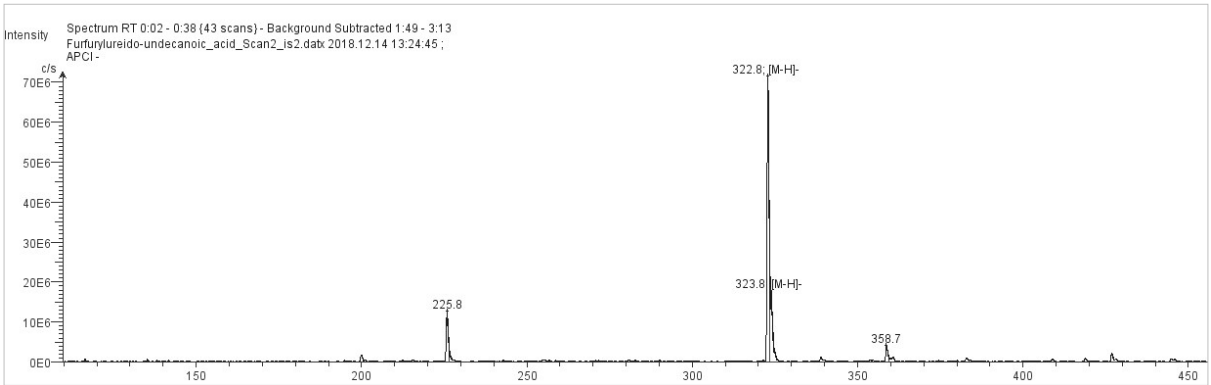

Figure S8. Mass spectrum of 11-(furfurylureido)undecanoic acid ($APCI^-$, $C_{17}H_{28}N_2O_4$, m/z).

Ligand exchange protocol and characterization of functionalized NPs

100 mg of $CoFe_2O_4$ NPs was dispersed in 20 mL of DCM and separated to two equal fractions (particles **A** and **B**). To the particles **A**, 20 mg of 11-maleimidoundecanoic acid was added and to the particles **B**, 23 mg of 11-(furfurylureido)undecanoic acid with 1 mL of methanol was added, which in both cases corresponds to about 2 eq. of the new ligand with respect to the oleic acid content. The reaction mixtures were sonicated for 5 minutes and then allowed to react in a closed vessel for 24 hours at room temperature. Then *n*-hexane was added to each fraction to precipitate the particles which were collected with a magnet, decanted and redispersed in DCM. The whole purifying process was repeated three times to remove the excess of ligands. Finally, the resulting NPs in the fractions **A** and **B** were dispersed in DCE and MeOH/DCE (1:3, v/v), respectively, to have the same concentration of 0.05 mg/mL. **DLS**: 12.20 ± 1.75 nm (particles **A**), 11.83 ± 0.10 nm (particles **B**). **IR** (KBr): Particles **A**, ν(cm^{-1}) = 2909 (m, CH_2), 2840 (m, CH_2), 1701 (s, C=O), 1463 (m, NCH_2), 1403 (m, C=C), 825 and 690 (2x s, CH), 600 (br s, Fe–O), 420 (br s, Fe–O). Particles **B**, ν(cm^{-1}) = 3327 (m, NH), 3120 (w, CH), 2910 (m, CH_2), 2845 (m, CH_2), 1709 (m, ureido C=O), 1610 (s, carboxy C=O), 1581 (s, C=C), 900 (m, CH), 808 (s, CH), 600 (br s, Fe–O), 420 (br s, Fe–O).

NPs functionalized with 11-maleimidoundecanoic acid (Particles A)

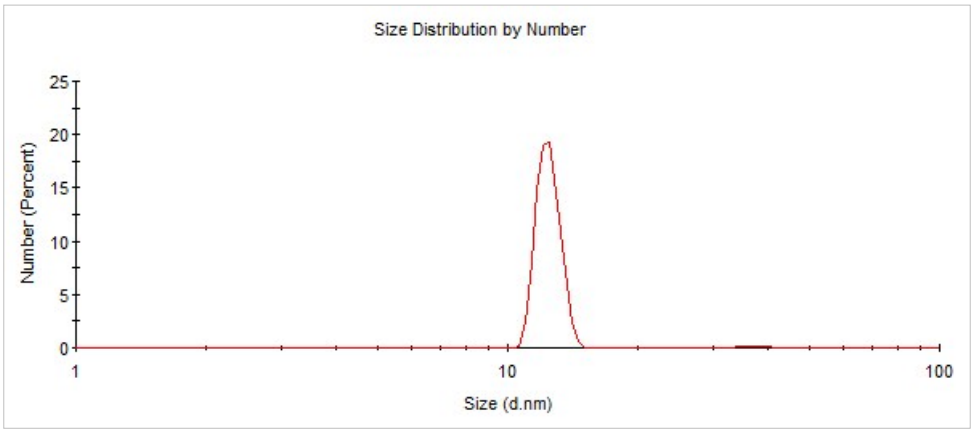

Figure S9. DLS spectrum of cobalt ferrites functionalized with 11-maleimidoundecanoic acid (DCE, 298 K).

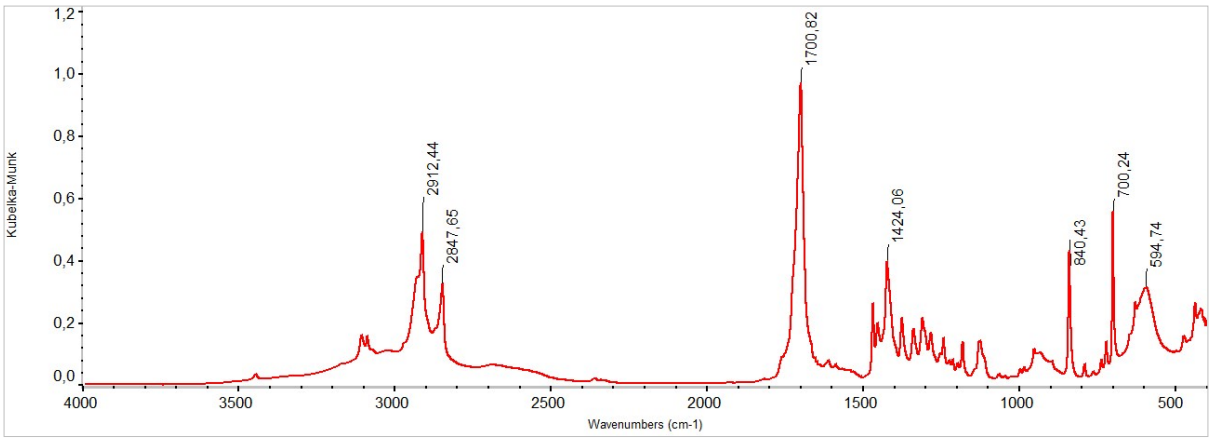

Figure S10. DRIFTS spectrum of cobalt ferrites functionalized with 11-maleimidoundecanoic acid (KBr, 298 K).

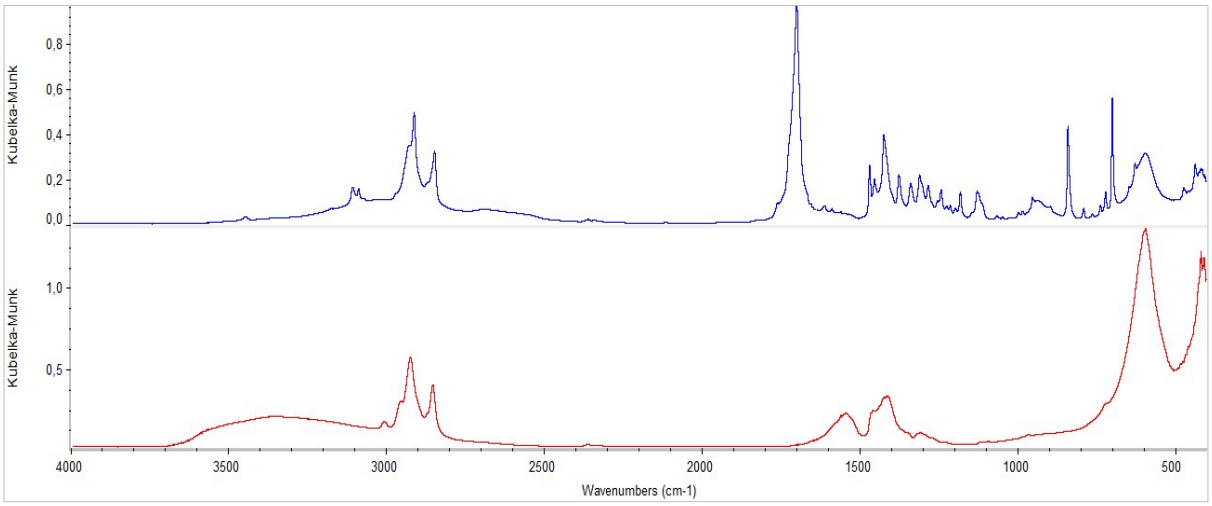

Figure S11. Comparison of IR spectra of cobalt ferrite oleates (red) and CoFe functionalized with 11-maleimidoundecanoic acid (blue).

NPs functionalized with 11-(furfurylureido)undecanoic acid (Particles B)

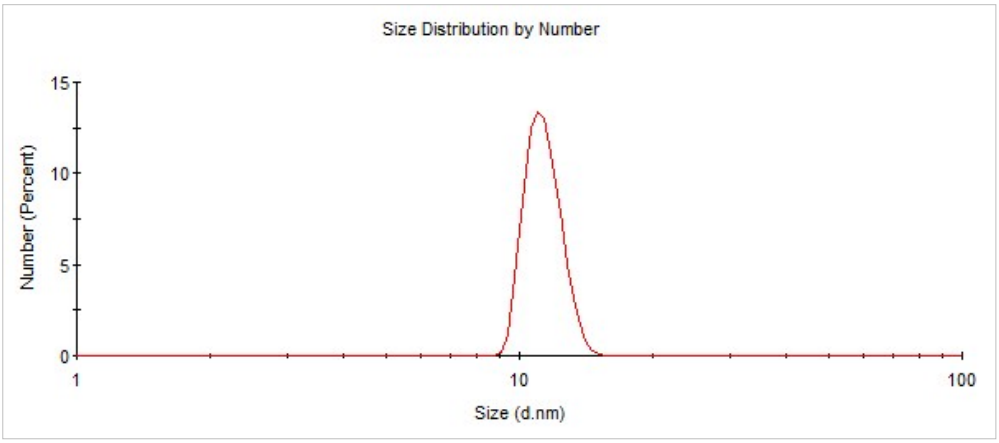

Figure S12. DLS spectrum of cobalt ferrites functionalized with 11-(furfurylureido)undecanoic acid (DCE, 298 K).

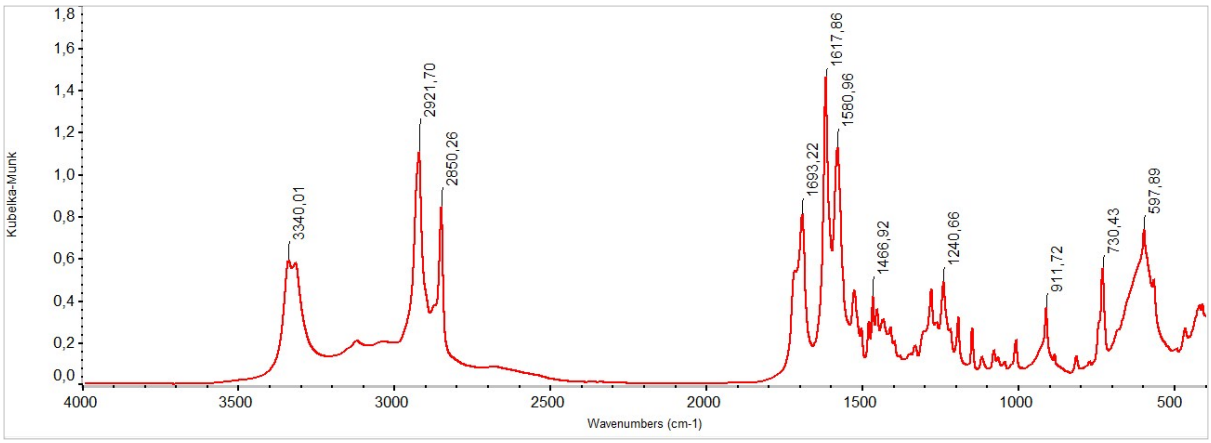

Figure S13. DRIFTS spectrum of cobalt ferrites functionalized with 11-(furfurylureido)undecanoic acid (KBr, 298 K).

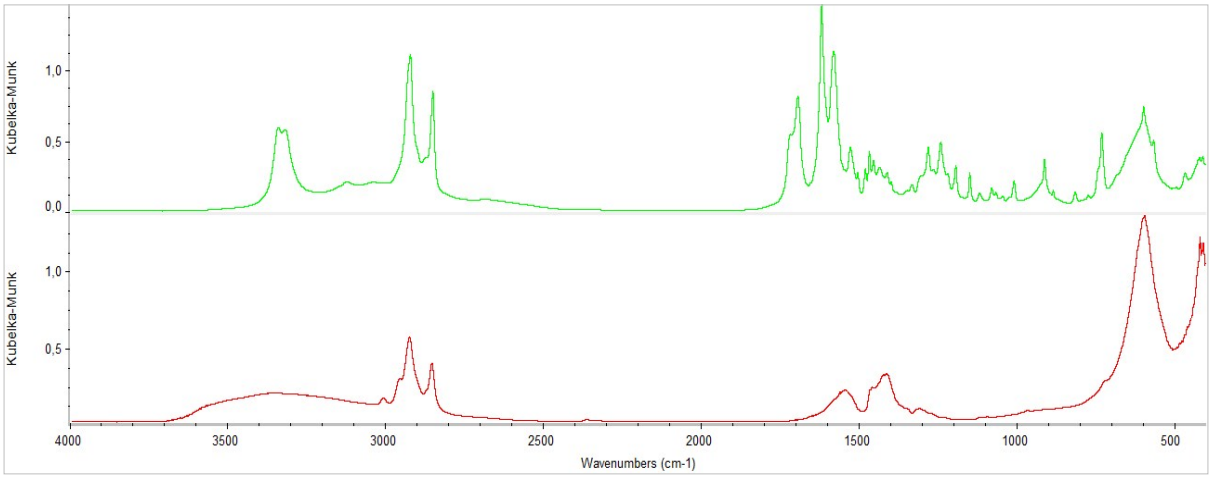

Figure S14. Comparison of IR spectra of cobalt ferrite oleates (red) and CoFe functionalized with 11-(furfurylureido)undecanoic acid (green).

Model Diels-Alder reaction

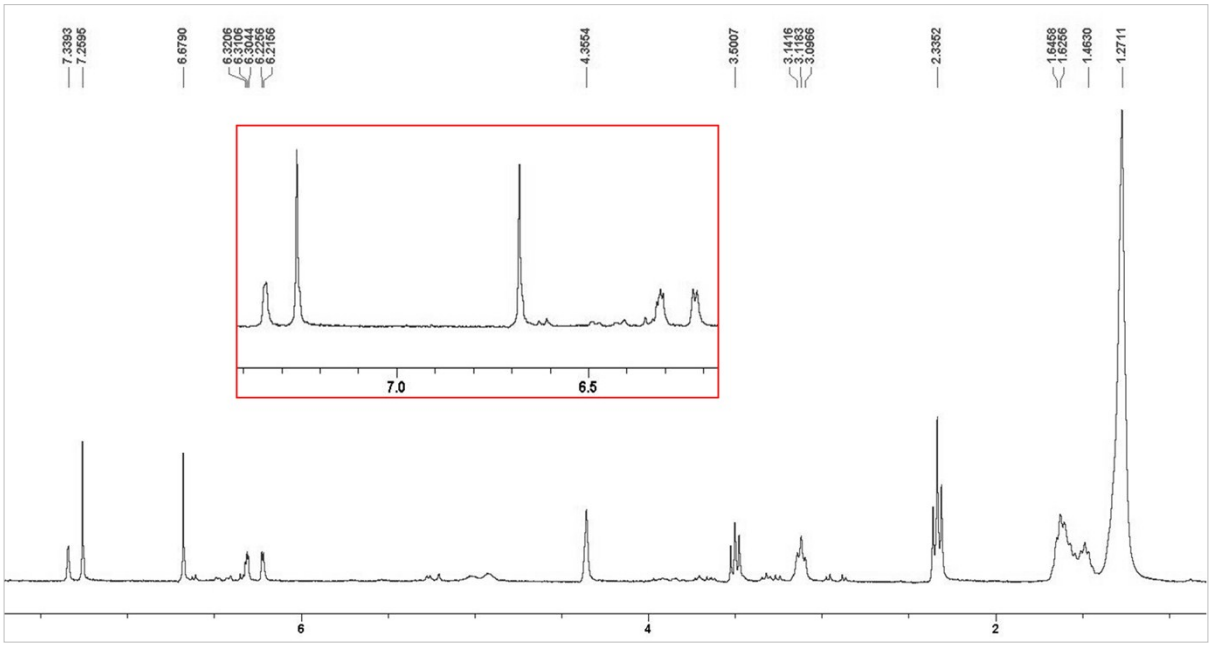

Figure S15. ^{1}H NMR of the Diels-Alder reaction between 11-(furfurylureido)undecanoic acid and 11-maleimidoundecanoic acid with the inset of aromatic region (t = 30min, 300 MHz, $CDCl_3$, 298 K, ppm).

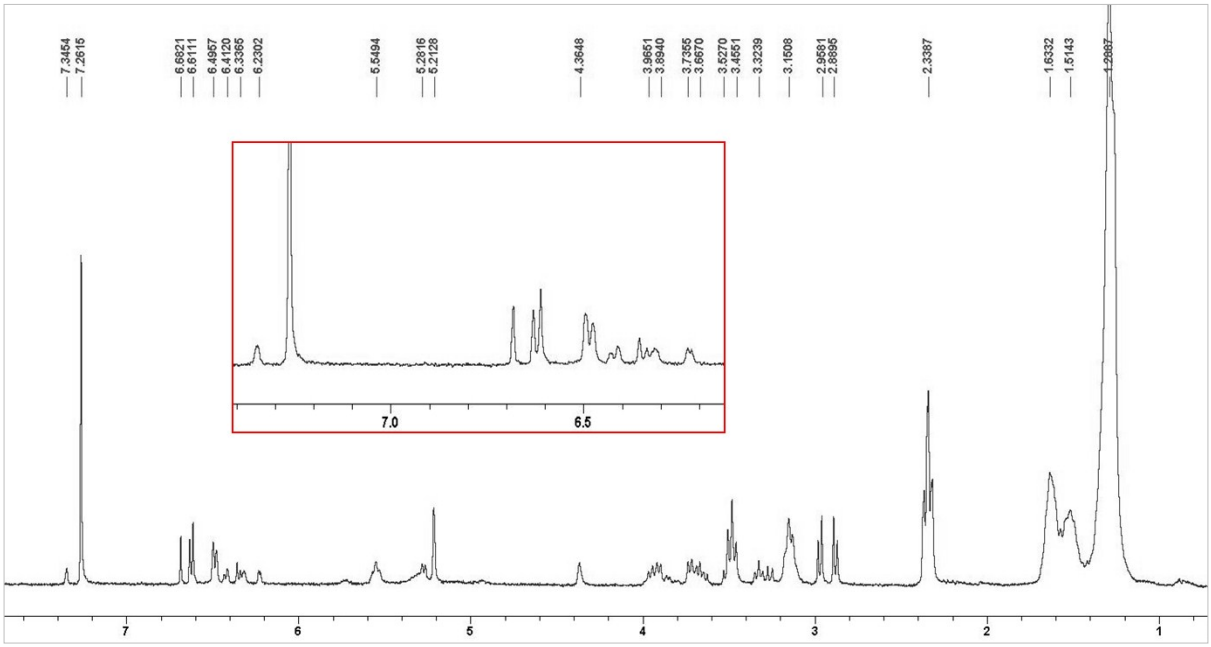

Figure S16. ^{1}H NMR of the Diels-Alder reaction between 11-(furfurylureido)undecanoic acid and 11-maleimidoundecanoic acid with the inset of aromatic region (t = 168 h, 300 MHz, $CDCl_3$, 298 K, ppm).

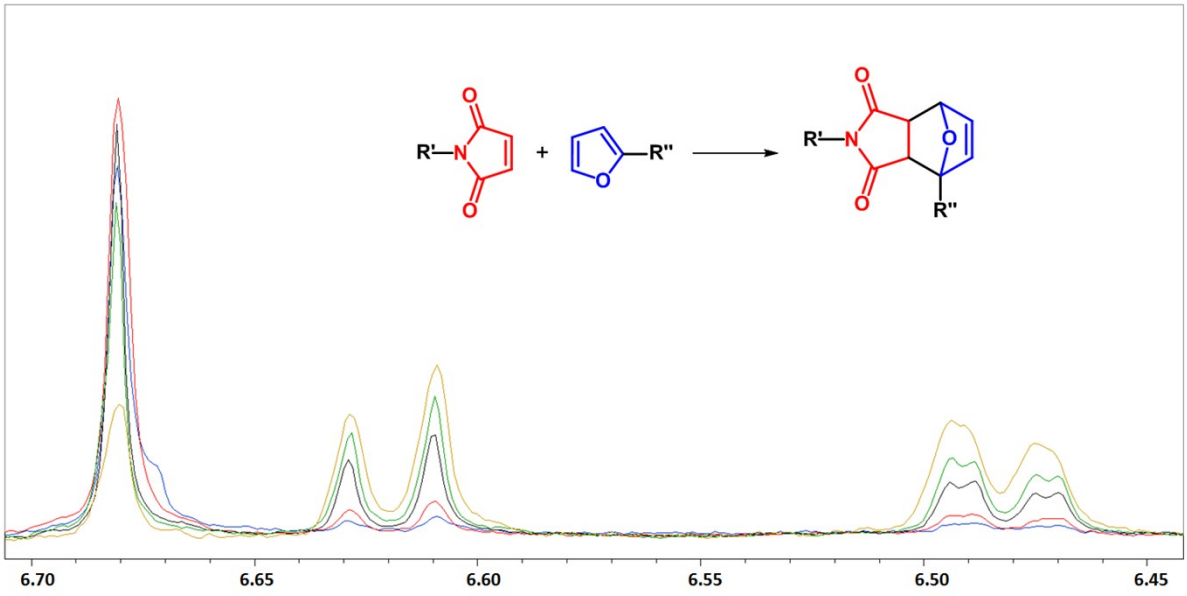

Figure 17. ^{1}H NMR spectra after 2 (blue), 4 (red), 24 (black), 48 (green) and 168 (yellow) hours with decreasing singlet of 11-maleimidoundecanoic acid (6.68 ppm) and increasing doublets (6.67 and 6.48 ppm) of the new double bond ($CDCl_3$, 298 K, 6.70–6.45 ppm).

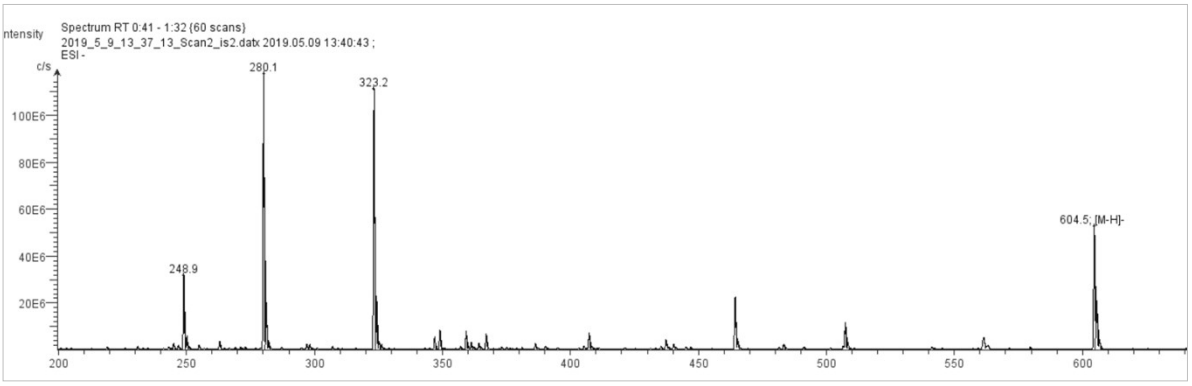

Figure S18. Mass spectrum (ESI^-) of the reaction mixture after 168 hours with the peaks of unreacted ligands (m/z 280.1, 11-maleimidoundecanoic acid and m/z 323.2, 11-(furfurylureido)undecanoic acid) and the product at m/z 604.5.

Diels-Alder reaction between the functionalized cobalt ferrites

DRIFTS spectra after magnetic-field-unassisted reaction

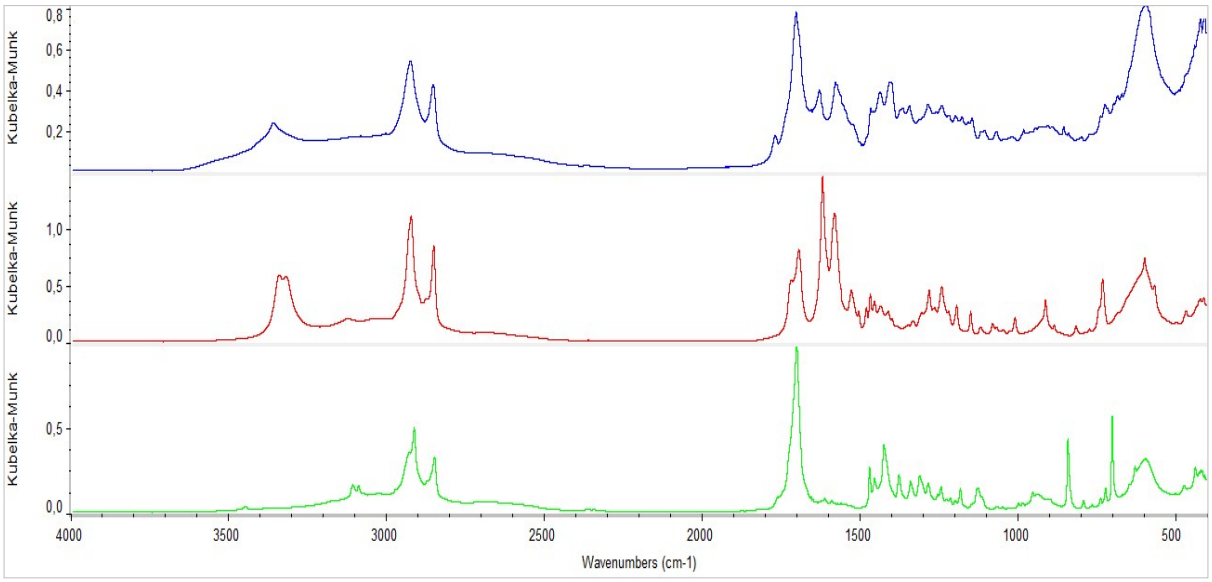

Figure S19. DRIFTS spectra of cobalt ferrite nanochains (blue) and a comparison with cobalt ferrites functionalized with 11-maleimidoundecanoic acid (green) and 11-(furfurylureido)undecanoic acid (red).

Diels-Alder reaction in the MF

The equal mixture (conc. 0.05 mg/mL) of particles **A** and **B** in a closed vial was placed with a home-made sample holder inside the cryomagnetic system (Physical Property Measurement System - PPMS, Quantum Design, Inc.; 6000 model series). A summary on the preparation conditions is given in **Table 1**. Once the reaction sequence was completed, the vial was removed from the PPMS system and a droplet of the resulting sample was placed immediately on TEM grids for further analysis. Part of the product was dried at room temperature for 24 hours and subjected to XRD and magnetic characterization. A summary of the tested preparation protocols for the MF-assisted reaction are given in **Table 1**.

Sample 1	***Sample 2***	***Experimental conditions setup.***
A	B	- > 300 to 330 K at 1 K/min -> 0 to 1T at 10 Oe/s -> *2 h* under 1 T DC field at 330 K -> Back to 300K and 0 T at the same previous rates.
A	B	- > 300 to 330 K at 1 K/min -> 0 to 1T at 10 Oe/s -> *12 h* under 1 T DC field at 330 K -> Back to 300K and 0 T at the same previous rates.
A	B	- > hold at 300 K-> 0 to 1 T at 10 Oe/s -> *2 h* under 1 T DC field at 300 K

		-> Back to 0 T at the same previous rate.
A	B	- > 300 to 330 K at 1 K/min -> 0 to 0.1 T at 10 Oe/s -> *4 h* under 0.1 T DC field at 330 K -> Back to 300 K and 0 T at the same previous rates.
A	B	- > 300 to 330 K at 1 K/min -> 0 to 1 T at 10 Oe/s -> *4 h* under 1 T DC field at 330 K -> Back to 300 K and 0 T at the same previous rates.
A	B	- > 300 to 330 K at 1 K/min -> 0 to 0.1 T at 10 Oe/s -> 12 *h* under 0.1 T DC field at 330 K -> Back to 300 K and 0 T at the same previous rates.
A	B	- > 300 to 330 K at 1 K/min -> 0 to 0.5 T at 10 Oe/s -> 12 *h* under 0.5 T DC field at 330 K -> Back to 300 K and 0 T at the same previous rates.

Table S1: Different conditions tested for the click reaction attempts.

DRIFTS spectra after magnetic-field-assisted reaction

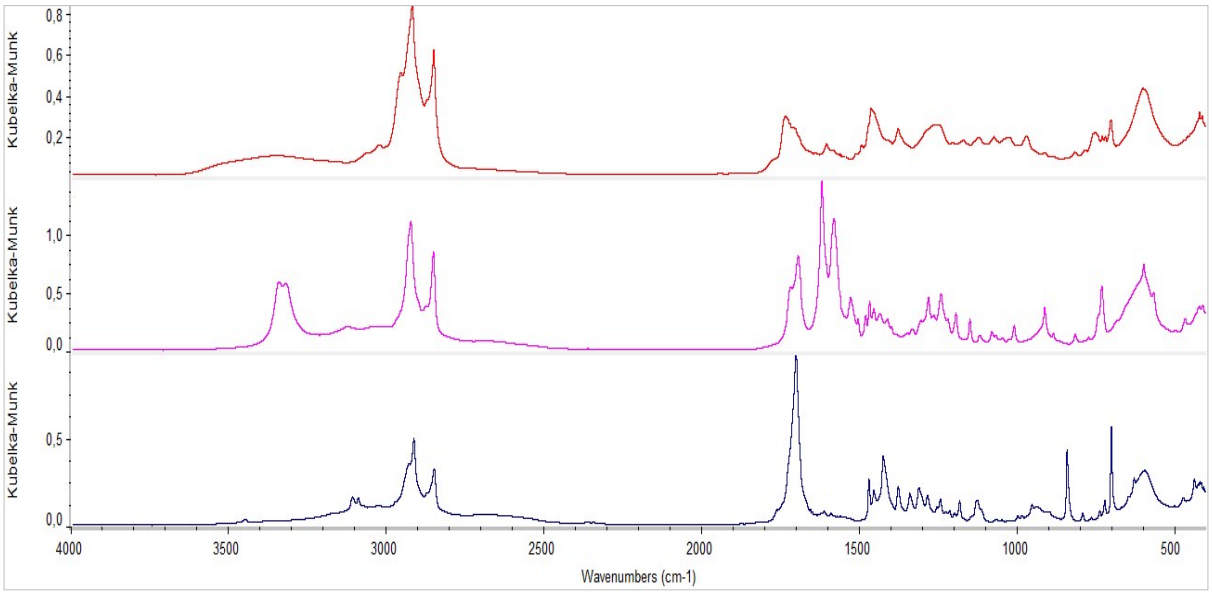

Figure S20. DRIFTS spectra of cobalt ferrite nanochains (red) and a comparison with cobalt ferrites functionalized with 11-maleimidoundecanoic acid (blue) and 11-(furfurylureido)undecanoic acid (purple).

Retro-Diels-Alder

The DCE dispersion (1 mL) of nanochains in a tightly closed vial was put into an autoclave and heated up to 115 °C for 12 hours. The samples were analyzed by HRTEM and DLS analyses.

HRTEM images after magnetic-field-(un)assisted Diels-Alder and *retro*-Diels-Alder reaction

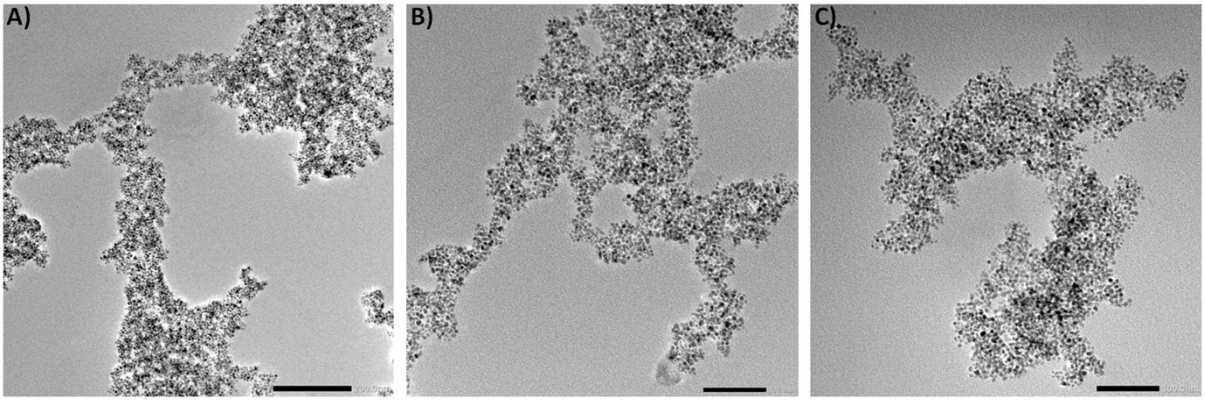

Figure S21. HRTEM images of assembled nanoparticles after magnetic-field-unassisted Diels-Alder reaction (scale bars = **a)** 200 nm; **b-c)** 100 nm).

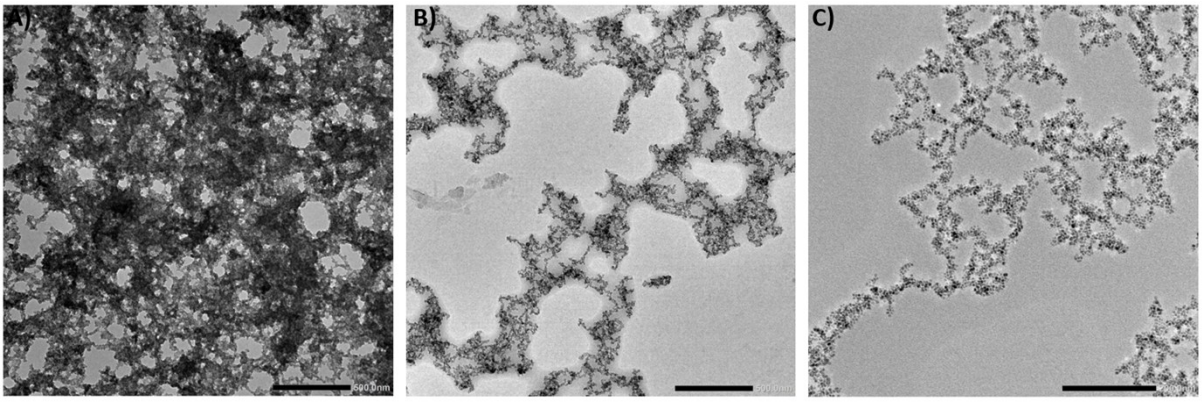

Figure S22. HRTEM images of **a)** large aggregates after the reaction with a high concentration of NPs (0.5 mg/mL), **b)** and **c)** branched chains after the reaction with NPs concentrations higher than 0.05 mg/mL (scale bars = **a-b)** 500 nm; **c)** 200 nm).

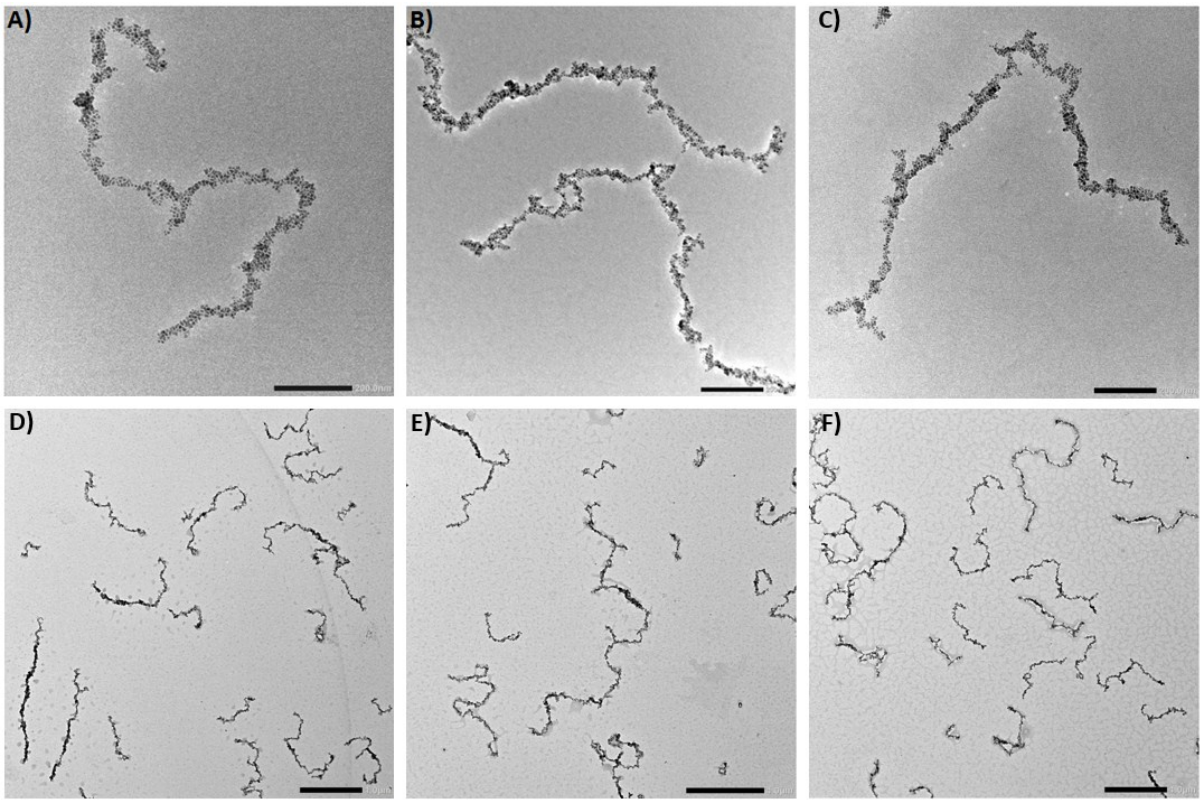

Figure S23. a-c) HRTEM images of covalently linked chains after magnetic-field-assisted Diels-Alder reaction (scale bars = 200 nm), **d-f)** representative large-scale HRTEM images of narrow chains (concentration 0.05 mg/mL, scale bars = 1 µm).

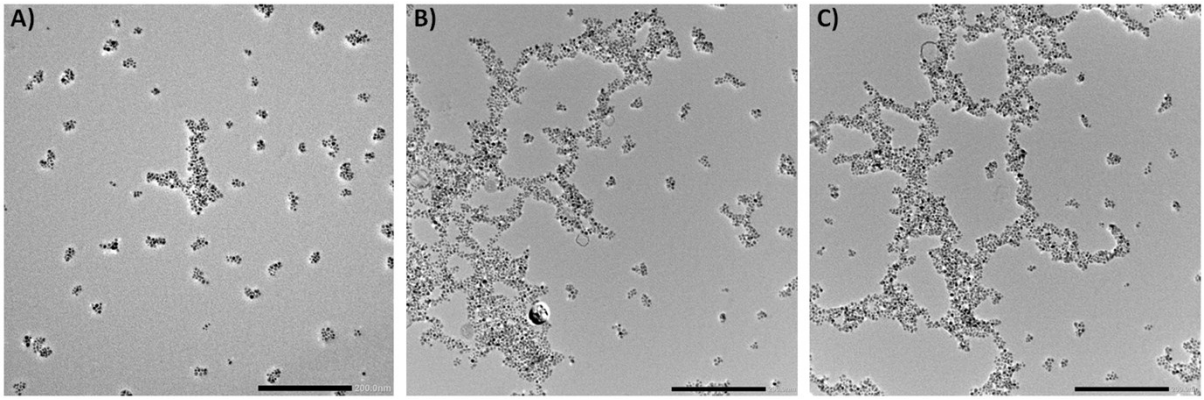

Figure S24. HRTEM images of resulting mixtures after magnetic-field-assisted Diels-Alder reaction with either too short reaction time or too low reaction temperature (scale bars = 200 nm).

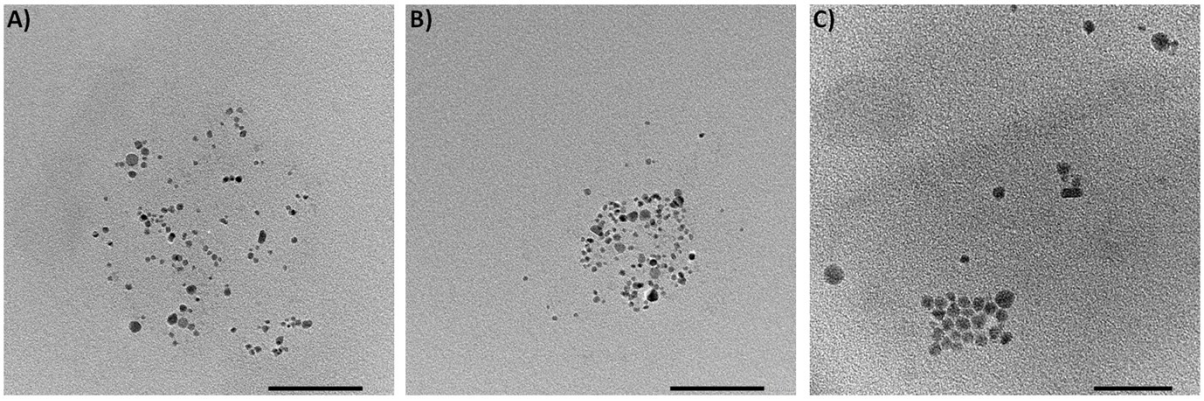

Figure S25. HRTEM images of disconnected chains after heating at 115 °C for 12 hours (scale bars = **a-b)** 100nm, **c)** 50 nm).

Magnetic measurements and properties

The magnetic susceptibility graph presented on the main text was determined using the following formula:

$$\chi = \frac{M * M_m}{B * \frac{1}{\mu_0} * 10^{-4}} \ (m^3 mol^{-1}),$$

where, χ is the molar susceptibility, M the mass magnetization in Am^2kg^{-1}, M_m the molar mass in $kg.mol^{-1}$, B the magnetic field in Oe and μ_0 the magnetic permeability in $H.m^{-1}$.

In this work, we used the differential method[3], which uses both measurements of the ZFC and FC susceptibilities. The blocking temperature is determined by first subtracting the FC susceptibility (χ_{FC}) from the ZFC susceptibility (χ_{ZFC}) and then finding the maximum of the derivative of the subtraction. The distribution of magnetic moment were determined using the non-regularized inversion method[4] by the MINORIM[4] software. Using the average magnetic dipole moment of the NPs it is possible to determine their 'magnetic size' by means of the following expression:

$$d_{MAG} = 2\sqrt[3]{\frac{3\ \mu_m}{4\pi\mu_{uc}} V_{uc}}$$ (in units of the volume cell V_{uc}),

where; d_{MAG} corresponds to the NP magnetic size (diameter), V_{uc} stands for the unit cell volume (a = 8.392×10^{-10} m for $Fe[CoFe]O_4$), μ_m is the mean magnetic moment and μ_{uc} is NP unit cell magnetic moment.

	H_c 10 K (T)	H_c 300 K (T)	M_s 10 K (Am^2/kg)	M_s 300 K (Am^2/kg)	M_r 10 K (Am^2/kg)	M_r 300 K (Am^2/kg)	Sq 10 K	Sq 300 K	T_B (K)
Sample **A**	1.20	≈0	64	55	42	≈0	0.66	-	164
Sample **B**	1.14	≈0	72	60	46	≈0	0.64	-	174
Oleic cores	0.80	≈0	82	65	48	≈0	0.59	-	152

Table S2. Values of the coercivity field (H_c), saturation magnetization (M_S), remnant magnetization (M_r), squareness of the isotherm ($S_q = M_r/M_S$), and blocking temperature (T_B).

	Normal spinel, μ_{uc} = 56 μB	Inverse spinel, μ_{uc} = 24 μB
Sample **A,** d_{MAG} (nm)	3.5	4.7
Sample **B,** d_{MAG} (nm)	3.7	4.9
Oleic cores, d_{MAG} (nm)	3.4	4.5
Chains, d_{MAG} (nm)*	4.7	6.2

Table S3: Magnetic size, $d_{MAG,}$ of the NPs if considering normal or inverse spinel. *Calculated after correction to paramagnetic contribution.

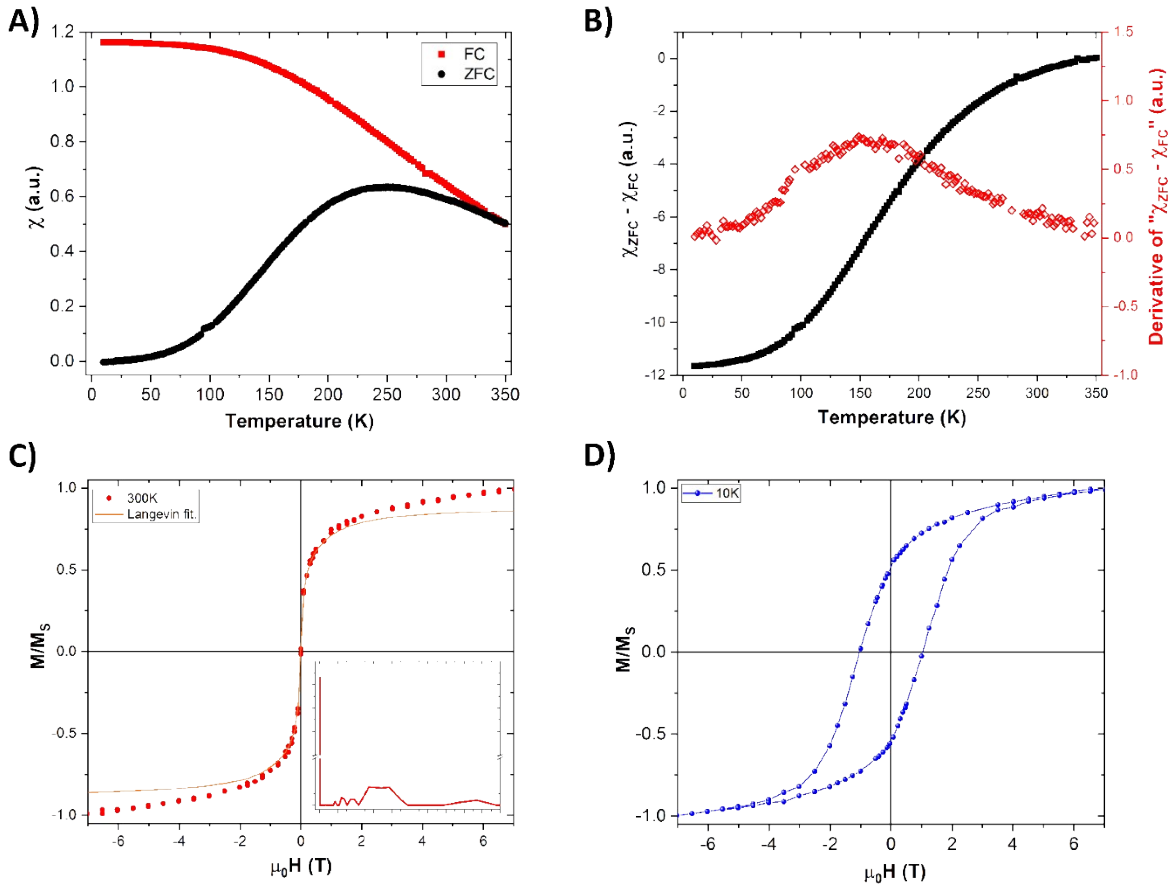

Figure S26. Magnetic measurments from the formed chains in powder form. **a)** ZFC and FC susceptibility under a field strength of 100 Oe. **b)** Determination of the blocking temperature; maximum of the derivative (open scatter lines) of the subtraction of the FC susceptibility (χ_{FC}) from the ZFC susceptibility (χ_{ZFC}), (solid scatter lines). **c)** Magnetic isotherm at 300 K showing typical superparamagnetic behaviour and corresponding Langevin fit with diamagnetic correction, performed on MINORIM; (magnetic moment distribution in inset). **d)** Magnetic isotherm at 10 K showing coercivvity fields ≈1.06 T.

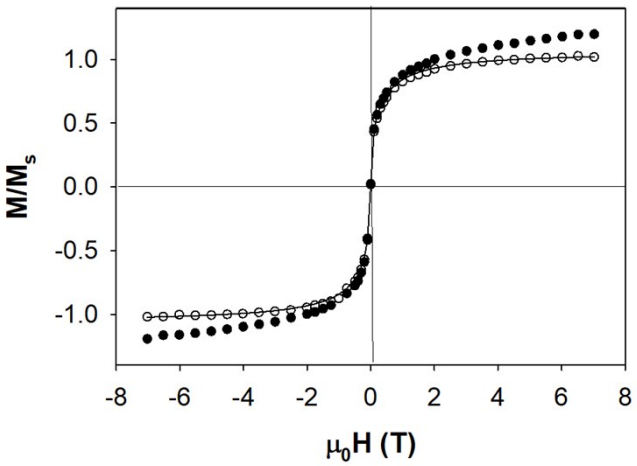

Figure S27. Magnetization isotherm of the chain sample. The solid circles correspond to the experimental data, the open circles to the data corrected to paramagnetic term and the solid line corresponds to the fit in MINORIM. The data were normalized after subtraction of the paramagnetic term.

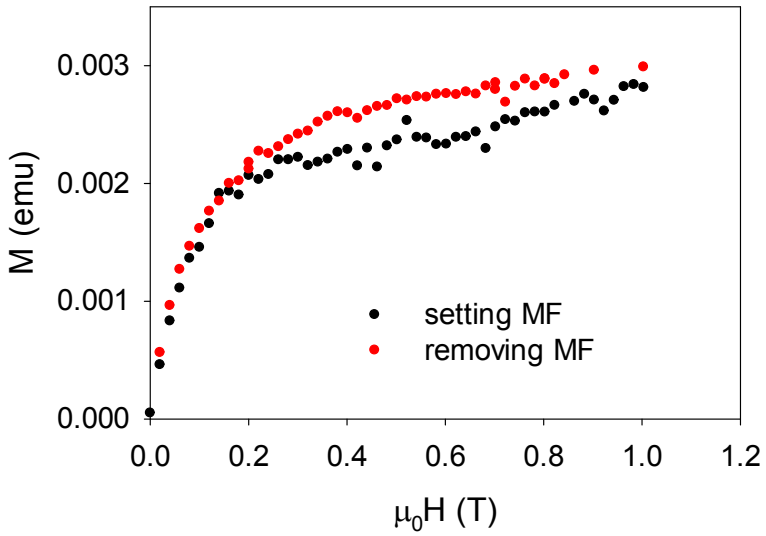

Figure S28. Monitoring of the magnetic signal of a NP dispersion during setting the magnetic field of 1 T and when removing the magnetic field.

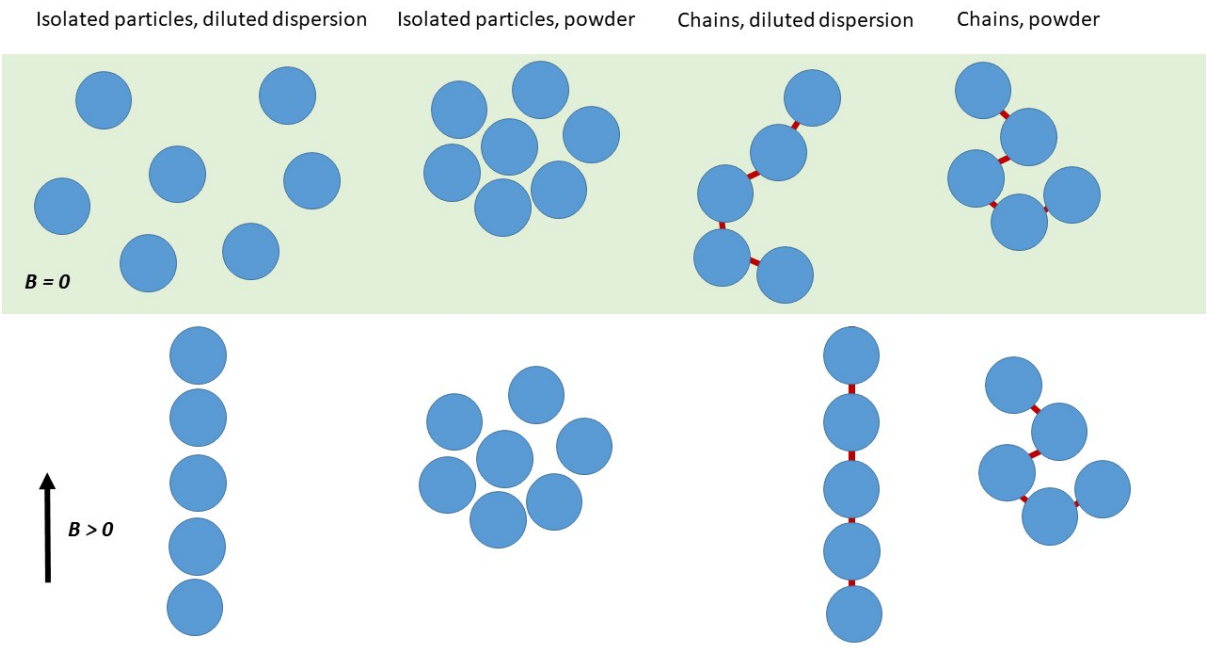

Figure S29. Schematic representation of the NP and chain packing in dispersion and powder in zero and elevated MF, respectively.

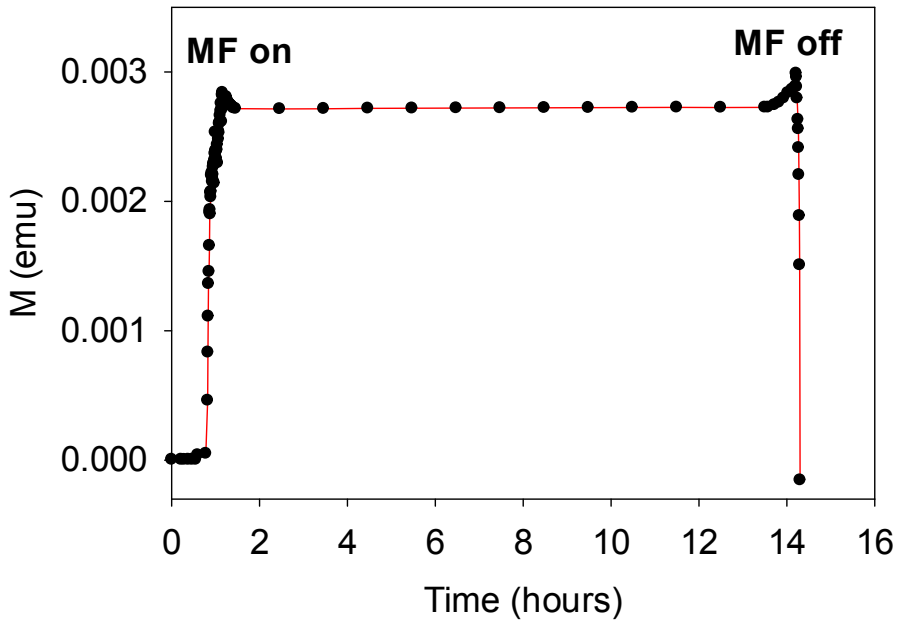

Figure S30. Monitoring of the magnetic signal of a NP dispersion during the MF-assisted click chemistry procedure.

Powder X-ray diffraction

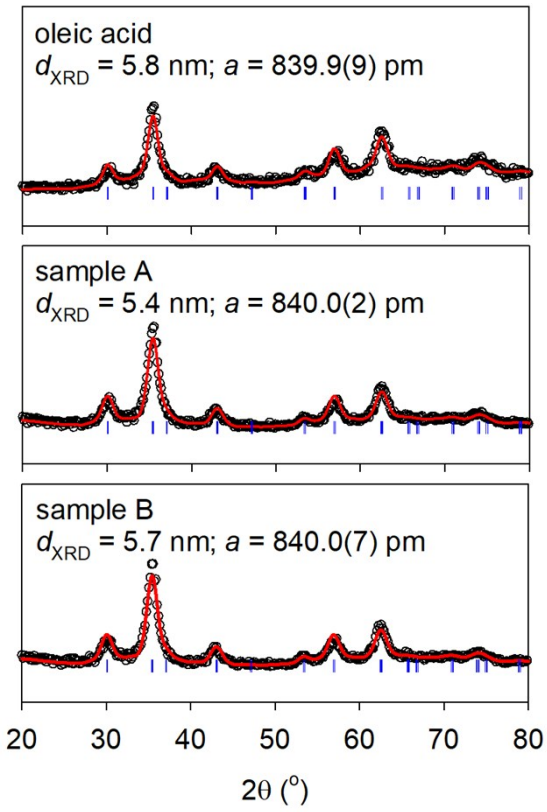

Figure S31. PXRD pattern and Rietveld fit of the $CoFe_2O_4$ cores. The estimate of the particle diameter, d_{XRD} (related to the size of the coherently diffracting domain with spherical symmetry) and lattice parameter of the cubic spinel structure is also given.

References

(1) T. Roisnel and J. Rodríguez-Carvajal WinPLOTR: a Windows tool for powder diffraction patterns analysis Materials Science Forum, Proceedings of the Seventh European Powder Diffraction Conference (EPDIC 7), 2000, p.118-123, Ed. R. Delhez and E.J. Mittenmeijer

(2) Repko, A.; Nižňanský, D.; Poltierová-Vejpravová, J. . *J. Nanoparticle Res* **2011**, *13* (10), 5021–5031.

(3) Bruvera, I. J.; Mendoza Zélis, P.; Pilar Calatayud, M.; Goya, G. F.; Sánchez, F. H. *J. Appl. Phys.* **2015**, *118* (18), 184304.

(4) van Rijssel, J.; Kuipers, B. W. M.; Erné, B. H. *J. Magn. Magn. Mater* **2014**, *353*, 110–115.

(5) Rijssel, J. van; Kuipers, B. W. M. MINORIM Inversion Method, 2018.